A STUDY ON THE POTENTIAL SAFETY ADVANTAGE OF LARGE HETEROGENEOUS LMFBRS

K. Suzuki, K. Miyagi and K. Aoki
Nippon Atomic Industry Group Co., Ltd.
4-1, Ukishima-cho, Kawasaki-ku, Kawasaki-city, Japan 210

T. Inoue and N. Ohtani
Power Reactor and Nuclear Fuel Development Corporation
1-9-13, Akasaka, Minato-ku, Tokyo, Japan 107

ABSTRACT

The potential safety advantage of large heterogeneous LMFBRs in hypothetical core disruptive accidents has been studied in contrast with that of the conventional homogeneous LMFBRs. The main objective of this study is to investigate the inherent safety features during accident sequences through comparison between the two types of cores. Neutronically optimized 1000 MWe heterogeneous and homogeneous cores have been designed on the same technological basis. The heterogeneous core designed here is characterized by the adoption of 6 mm pellet diameter, 80 cm core height and island-type configuration resulting in a very low sodium void reactivity. Safety analyses for loss-of-flow and transient over-power accidents were made using the SAS3D and VENUS codes. As a result of this study, it was found that the heterogeneous core studied here has smaller possibility of reaching prompt critical and that even if it should reach prompt critical by the adoption of very conservative assumptions, the resulting work energy may be about a half that of the homogeneous core. It is concluded that the heterogeneous core with a lower void reactivity has a significant advantage for accommodating the energetics issues over the homogeneous core, when rather conservative assumptions are employed for the analysis.

INTRODUCTION

The potential safety advantage of large heterogeneous LMFBRs in hypothetical core disruptive accidents (HCDAs) has been studied in contrast with that of the conventional homogeneous LMFBRs.
The objectives of the present study are : (1) to investigate the potential safety advantage of the heterogeneous core and (2) to compare the accident sequences in both types of cores through HCDA scenario.
In the preceding preliminary investigations [1 - 5], it was found that it is very difficult to discuss the general safety advantage of the heterogeneous cores because the analytical results might be strongly influenced by the difference of core designs. This report describes the design of new heterogeneous core and presents the results of accident analysis by the SAS3D code.

CORE DESIGN

Our previous research [1,2] was performed for large 1000 MWe cores designed with the same technological basis as that of a prototype LMFBR. With the core height of 100 cm, the maximum core void reactivities at the end-of-equilibrium cycle (EOEC) were 3.4 $ for the heterogeneous (HE) core and 5.2 $ for the homogeneous (HO) core. As for the related safety studies, HCDA analyses for loss-of-flow (LOF) and transient over-power (TOP) accidents were made using rather simple and conservative computational models. In these studies, any definite conclusion on the safety advantage of the HE core over HO counterpart could not be drawn because of rather large void reactivity coefficient of the HE core and the employment of most pessimistic assumptions such as fuel compaction. However, it was predicted that the threshold value of core void reactivity to insist the advantage of HE cores would be 2~2.5 $.

In our present research, the optimization of neutronics design has been directed toward attaining shorter doubling time and smaller sodium void reactivity coefficient. As a result of this study, a set of optimum parameters (6 mm pellet diameter, 80 cm core height and island-type configuration) were selected. The HO counterpart was also designed with the same fuel dimensions and the same maximum linear heat rate criteria (430 W/cm).

The layouts of the HE and HO cores are shown in Fig. 1. Design parameters and neutronic characteristics at EOEC of both cores are listed in Tables 1 and 2, respectively. For the HE core, there are 378 fuel assemblies and 157 internal blanket assemblies, and there are 433 fuel assemblies for the HO core. With introduction of the internal blanket assemblies, the equivalent diameter of core is larger by about 40 cm in the HE core than in the HO core. The breeding ratio and compound system doubling time (assumung 2 % loss and 1.5 years for out-of-reactor time) are 1.32 and 25 years for the HE core, and 1.23 and 29 years for the HO core. The maximum core void reactivities are 2.3 $ for the HE core, which fulfills the aforementioned predicted safety criteria, and 4.3 $ for the HO core.

SAS3D CHANNELING

The analysis codes used for the accident simulation are the SAS3D [6] for the initiating phase and the VENUS [7] for the disassembly phase.

The criteria for grouping assemblies into SAS3D channel is based on the following considerations : (1)assembly type (core or blanket), (2) power level, (3) power-to-flow ratio and (4) assembly location. The grouping by fuel burnup is not considered in this study, and this procedure is seemed to be conservative assumption in respect of the coherency of fuel pin failure. The HE and HO cores were divided into 16 and 14 channels, respectively.

Figure 2 shows the average bundle power and relative power-to-flow ratio for each channel in both cores. The peak of the relative power-to-flow appears in channel 10 in the HE core and in channel 2 in the HO core, respectively. The reactivity worth distridution of sodium void

is shown in Fig. 3 for both cores. The void reactivity worth per bundle of the HE core is much smaller and has much flatter radial distribution than that of the HO core. The density coefficient distribution of fuel for each channel is shown in Fig. 4. The HE core has larger values and axially sharper distribution of fuel density coefficients. Therefore, the reactivity change due to fuel motion is larger in the HE core.

By shortening the fissile core height from 100 cm to 80 cm, much lower void reactivity can be obtained and a larger nagative reactivity can be expected due to fuel dispersion out of the core.

PHYSICAL ASSUMPTIONS IN ACCIDENT ANALYSIS

Two types of situations were considered as the hypothetical accidents : LOF and TOP accidents under without-scram condition. The LOF accident was assumed to be induced by a loss of primary pumping power causing about 50 % reduction in coolant flow within 5 sec. The TOP accident was assumed to be induced by a control rod withdrawal causing the insertion of reactivity at a rate of 10 ¢/s.

The main physical assumptions in the BASE CASE were as follows:
- The reactivity feedback due to fuel axial expansion is neglected.
- Molten cladding motion is initiated when the cladding temperature reaches the melting point.
- The fuel motion and fuel-coolant interaction (FCI) are initiated when the molten fraction of fuel exceeds 50 %.
- Fuel disperses by the pressure of fission gas, steel vapor and its own vapor pressure.
- The mixing time of fuel in FCI is 10 msec.

Additional sensitivity studies were carried out to investigate the effect of key parameters: fuel axial expansion reactivity, fuel motion model and FCI behavior. Table 3 shows main parameter values in four cases. The degree of conservativeness in the phenomenological assumptions becomes large as the increase of the case number.

As for the safety criteria for clarifying the advantage, the following two items were adopted in this study: (1) the possibility of reaching super prompt critical and (2) the work energy produced from fuel vapor expansion to 1 atm during disassembly phase.

RESULTS OF ACCIDENT ANALYSIS

The steady state conditions were determined before transient analyses. The maximum fuel centerline temperatures are 1840 °C in channel of the HE core and 1829 °C in channel 2 of the HO core. The maximum coolant temperatures are 570 °C in the HE core and 573 °C in the HO core. The maximum temperatures of fuel and coolant in the internal blanket of the HE core are 1627 °C and 554 °C, respectively.

LOF Accident

Tables 4 and 5 show the summary of LOF accidents and the reactivity components at peak net reactivity, respectively.

The main results of the BASE CASE are as follows. Figure 5 compares power traces and accident sequences between HE and HO cores. The reactivity traces are shown in Fig. 6.

In the HE core, the sodium boiling occurs at about 16 sec in the hottest channel 10. The subsequent cladding relocation and fuel motion are initiated at 20.0 sec and 20.8 sec, respectively. The net reactivity reaches its peak of 0.95 $ at 20.9 sec and the normalized peak power reaches 64. The core does then become slightly subcritical because of slower insertion of void reactivity and larger negative reactivity due to fuel dispersion. The coolant in all internal blankets still remain subcooled. Therefore, only sodium void reactivity in the core region contributes to the positive reactivity during the initiating phase.

In the HO core, the sodium boiling occurs at about 15 sec in the hottest channel 2 and subsequent cladding relocation and fuel motion are initiated at 17.76 sec and 17.77 sec, respectively, in the inner core region. The core reaches super prompt critical at 17.78 sec by FCI taking place in the outer core region. The peak normalized power reaches 6626 and is about 100 times that of the HE core. The reactivity ramp rate peaks at about 70 $/s. The work energy produced from fuel vapor expansion to 1 atm is about 1040 MJ.

The sodium void reactivity inserted into the HE core is about 1.7 $ and 60 % lower than that of the HO core. The melt fraction of fuel in the core region is 15 % for the HE core and 80 % for the HO core. The time interval between the onset of sodium boiling and the initiation of fuel motion in the HE core is about 5 sec, while it is about 3 sec in the HO core. Therefore, the HE core accident would show slower propagation in sequences. Although the HO core follows the so-called LOF-driven TOP type scenario, which is characteristic of the accident in large LMFBR cores, the HE core shows the typical LOF type behavior.

In addition to the BASE CASE, parametric studies were carried out to investigate the effects of reactivity feedback due to fuel axial expansion (REALISTIC CASE), the fuel motion model (SLUMPING CASE) and the fuel motion/FCI behavior (PESSIMISTIC CASE).

In the REALISTIC CASE, in which the feedback reactivity due to fuel axial expansion is considered, both cores does not lead to super prompt critical. Figure 7 shows power traces of both cores for comparison. The peak normalized power of the HE core is at most 7 which is one-tenth that of the HO core. The peak net reactivity of the HE core is 0.73 $; so the HE core has large safety margin up to super prompt criticality compared with 0.94 $ in the HO core.

In the SLUMPING CASE, it was conservatively assumed that the fuel motion and FCI are initiated when the molten fuel fraction exceeds 25 % and the molten fuel falls at only the gravitational acceleration. The accident sequences and power traces are shown in Fig. 8. The fuel motion in the HE core takes place at 20.6 sec and is 0.2 sec faster than in the BASE CASE. The positive feedback reactivity due to fuel motion toward the core midplane induced FCI and results in super prompt critical at 20.7 sec. The normalized power peaks at 1174 and 18 times in the BASE CASE. The sequences of the HO core are almost similar to the HO BASE CASE, because the effect of feedback reactivity due to fuel motion is small compared with the large sodium void reactivity. The work energy of the HE and HO cores are about 500 MJ and 1140 MJ, respectively.

Though the coolant boiling occurs in the internal blanket assemblies in the SLUMPING CASE of the HE core, the positive void reactivity of internal blankets is not inserted until the reactor becomes substantially subcritical by the molten fuel ejection from the core.

The PESSIMISTIC CASE, which was further assumed to introduce the rapid FCI behavior in the SLUMPING CASE, results in more energetic excursion than other cases in both cores. The work energies for the HE and HO cores are about 700 MJ and 1270 MJ, respectively.

Figure 9 and Figure 10 depict the peak net reactivity and the work energy for each case in LOF accidents. Increasing the conservative degrees of phenomenological uncertainties, the possibility of super prompt critical becomes large and the work energy also become large. Those figures show that the HE core behaves consistently more milder than does the HO core.

TOP Accident

In the TOP accident, which was assumed to be similar to the BASE CASE in LOF accidents, both cores lead to early termination by the insertion of large negative reactivity due to fuel sweep-out caused by FCI behavior (shown in Table 6). The peak net reactivity is less than 0.4 $ for both cores. There appears no significant difference in the accident scenario.

CONCLUSIONS

HCDA analyses have been made with the SAS3D code to investigate the safety advantage of the HE core with a lower void reactivity. Main conclusions of the present study can be summarized as follows:

(1) The HE core studied in this work will not reach super prompt critical in the LOF accident if the fuel dispersion could be expected (BASE CASE), and on the other hand, the HO core will result in an energetic excursion under the same conditions.
(2) In the LOF case with the assumptions of the gravitational fuel motion and rapid FCI behavior (SLUMPING and PESSIMISTIC CASES), both cores will result in energetic excursions. However, the work energy in the HE core will be about a half that of the HO core.
(3) When the feedback reactivity due to fuel axial expansion and fuel dispersion can be expected, both cores will have very small possibility of reaching super prompt critical.
(4) The large void reactivity plays a dominant role in the HO accident sequences, and in the HE core with a lower void reactivity, the fuel motion would be very impotant phenomena.
(5) In the TOP case, the accidents will result in the early termination for both cores because of large negative reactivity due to fuel sweep-out by FCI. There appears no significant difference in the accident sequences between the two types of cores for the insertion rate as large as 10 ¢/s.

It can be deduced that a lower sodium void reactivity leads to a smaller possibility of core critical and a smaller work energy in the energetic phase. Therefore, it is concluded that the HE core designed here has a significant advantage over the HO counterpart in the event of hypothetical accidents.

ACKNOWLEDGMENTS

The SAS3D code is transmitted from USDOE and ANL/RAS to PNC under Special Memorandum of Agreement on LMFBR Safety. The authors wish to express gratitude to USDOE and ANL/RAS for making the code available.

The present work was performed at Nippon Atomic Industry Group Co., Ltd. (NAIG) under contracts with PNC and Toshiba Corporation.

REFERENCES

1. K. Miyagi et al., A Study on the Potential Safety Advantage of Large Heterogeneous LMFBRs (1), OECD NEACRP-A-357, The 22nd Meeting, 1979.
2. K. Miyagi et al., A Study on the Potential Safety Advantage of Large Heterogeneous LMFBRs (2), OECD NEACRP-A-484, The 24th Meeting, 1980.
3. T.A. Shih and M. I. Temme, An SAS3D Analysis of Unprotected Loss-of-Flow Transients for 1200 MW(electric) Liquid-Metal Fast Breeder Reactor Homogeneous and Heterogeneous Core Designs, Nucl. Tech., Vol 41, 1978.
4. Y. Balloffet et al., Calculation of the Loss of Flow Accident in Large LMFBR: Influence of Core Parameters, Proc. International Meeting on Fast Reactor Safety Technology, Seattle, Washington, 1979.
5. A. Renard et al., Comparative Study of Heterogeneous and Homogeneous Liquid-Metal Fast Breeder Reactor Cores in Some Accident Conditions, Nucl. Tech., Vol 46, 1979.
6. A Preliminary User's Guide to Version 10 of SAS3D.
7. W.T. Sha and T.H Hughes, VENUS: An Two-dimensional Coupled Neutronics-Hydrodynamics Computer Program for Fast-Reactor Power Excursions, ANL-1970, 1970.

Table 1 Design Parameters of Heterogeneous and Homogeneous Cores

Items		HE	HO
Reactor power	(MWt)	2400	2400
Reactor coolant temperature (°C) outlet/inlet		530/400	530/400
Total number of fuel assemblies in the core (IC/OC)*		378	433 (247/186)
Total number of blanket assemblies IB/RB *		157/288	0/252
Total number of control rod primary/secondary		24/12	24/6
Equivalent diameter of core	(cm)	379.9	342.1
Height of core	(cm)	80.0	80.0
Thickness of axial blanket upper/lower	(cm)	35.0/35.0	35.0/35.0
Volume of core	(l)	9068.0 **	7353.0
Core fuel pin			
pellet diameter	(cm)	0.6	0.6
cladding diameter inner/outer	(cm)	0.616/0.696	0.616/0.696
Maximum linear heat	(W/cm)	426.0	432.0
Breeding ratio		1.32	1.23
Compound system doubling time	(years)	25.1	28.9
Burnup	(MWD/T)		
maximum		106000	101800
average		73700	71500

* IC : Inner core
OC : Outer core
IB : Internal blanket
RB : Radial blanket

** including IB

Table 2 Neutronic Characteristics of Heterogeneous and Homogeneous Cores

Items	HE	HO
Sodium void reactivity ($)		
Regional total void reactivity		
core	1.94	3.97
internal blanket	1.29	----
radial blanket	-0.21	-0.27
axial blanket	-0.26	-0.30
total	2.76	3.40
Maximum void reactivity	2.27	4.23
core	2.27	4.23
internal blanket	1.29	----
total	3.56	4.23
Doppler reactivity coefficient ($-Tdk/dT \times 10^{-4}$)		
core (N/V)*	50.4/37.4	89.0/64.6
internal blanket	45.2/37.0	----------
radial blanket	6.5/ 5.8	2.9/2.1
axial blanket	15.2/15.5	15.7/12.9

* N : Normal core
V : Voided core

Table 3 Analysis Cases for LOF Accidents

case number	1	2	3	4
case name	realistic case	base case	slumping case	pessimistic case
Feedback reactivity due to fuel axial expansion	100 % considered	neglected	neglected	neglected
Fuel failure criteria (melt fraction)	50 %	50 %	25 %	50 %
Fuel motion model				
steel vapor pressure	considered	considered	neglected	neglected
fission gas pressure	considered	considered	neglected	neglected
gravitational force	considered	considered	considered	considered
FCI model				
fuel particle radius	117 μm	117 μm	117 μm	100 μm
fuel mixing time	10 msec	10 msec	10 msec	0 msec
rip length	15 cm	15 cm	15cm	5 cm

Table 4 Summary of Transient Analysis Results in LOF Accidents

	Realistic case		Base case		Slumping case		Pessimistic case	
	HE*	HO*	HE	HO	HE	HO	HE	HO
Initiating phase								
1) Peak value								
normalized power	7	79	64	6626	1174	4547	2726	5557
net reactivity ($)	0.73	0.94	0.95	1.16	1.03	1.12	1.06	1.12
reactivity ramp rate ($/s)	7.2	9.2	8.5	72.9	14.4	76.1	36.6	75.0
2) Onset of disassembly								
molten fuel mass (KG)	1647**		3107**	9261	14931	8984	16456	11997
molten fuel average temperature (°C)	2707**		2727**	2711	2980	2703	3247	2760
Disassembly phase								
duration of prompt critical state(ms)				4.4	1.3	3.4	1.3	1.6
total molten fuel mass (KG)				21775	19225	21830	20464	23075
molten fuel average temperature (°C)				3983	3713	4021	3760	4092
fuel vapor work energy to 1 atm (MJ)				1041	504	1139	694	1266

* HE : Heterogeneous core HO : Homogeneous core
** Value at peak net reactivity

Table 5 Reactivity Components at Peak Net Reactivity in LOF Accidents

	realistic case		base case		slumping case		pessimistic case	
	HE*	HO*	HE	HO	HE	HO	HE	HO
Reactivity component ($)								
net	0.73	0.94	0.95	1.16	1.03	1.12	1.06	1.12
Doppler	-0.91	-1.32	-1.07	-1.53	-1.61	-1.48	-1.64	-1.64
sodium void	1.86	3.17	1.69	2.65	1.73	2.50	1.33	2.60
cladding relocation	0.79	0.25	0.19	0.02	0.24	0.01	0.40	0.12
fuel motion	-0.39	-0.01	0.14	0.02	0.67	0.09	0.47	0.04
fuel expansion	-0.62	-1.13	0.0	0.0	0.0	0.0	0.0	0.0
Time of peak net reactivity (sec)	25.55	20.56	20.92	17.78	20.72	17.77	21.01	17.90

* HE : Heterogeneous core HO : Homogeneous core

Table 6 Summary of Transient Analysis in TOP Accidents

	HE*	HO*
Initiating Phase		
1) Peak Value		
Normalized Power	5.2	4.9
Net Reactivity ($)	0.43	0.38
Reactivity Ramp Rate ($/S)	20.1	9.6
2) Channel Number of Pin Failure	10 3	1 2

* HE : Heterogeneous Core
HO : Homogeneous Core

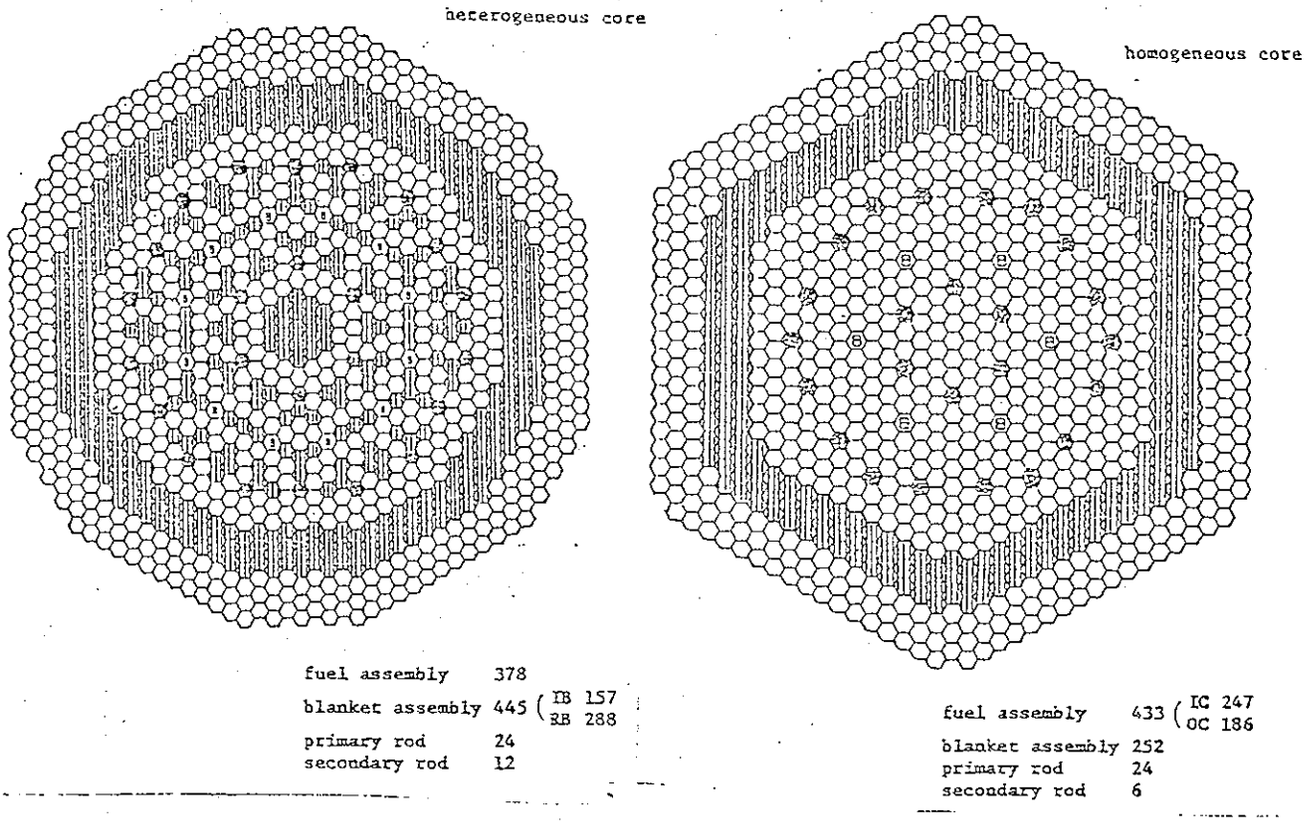

Fig. 1 Layouts of Heterogeneous and Homogeneous Cores

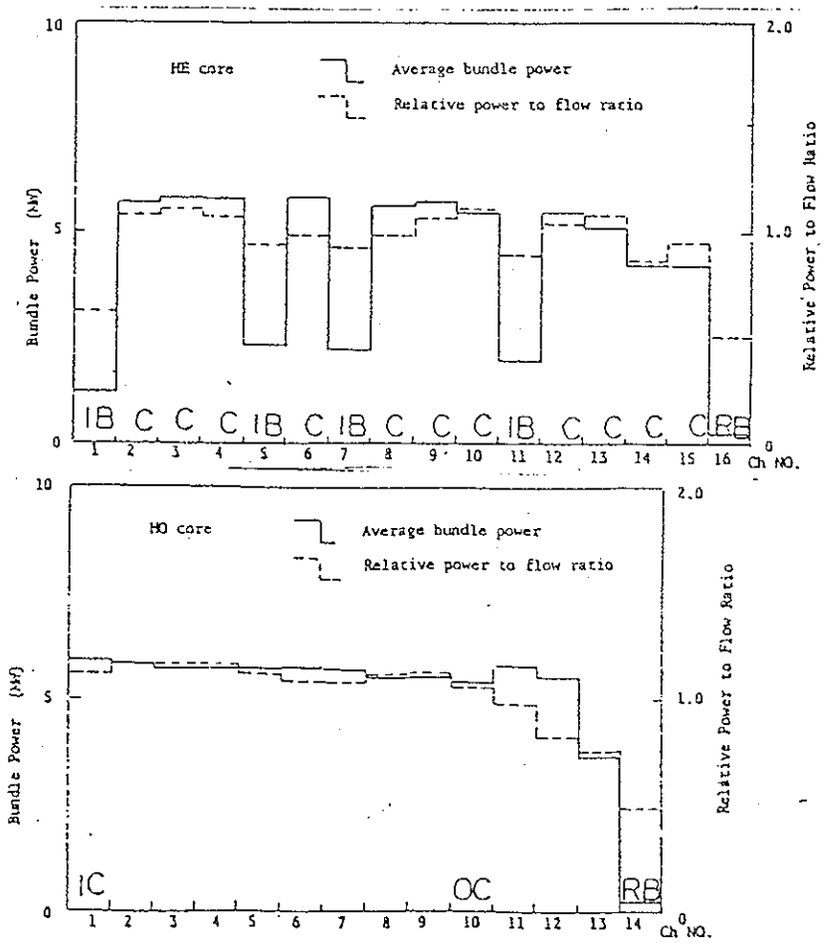

Fig. 2 Average Bundle Powers and Relative Power to Flow Ratios in Both Cores

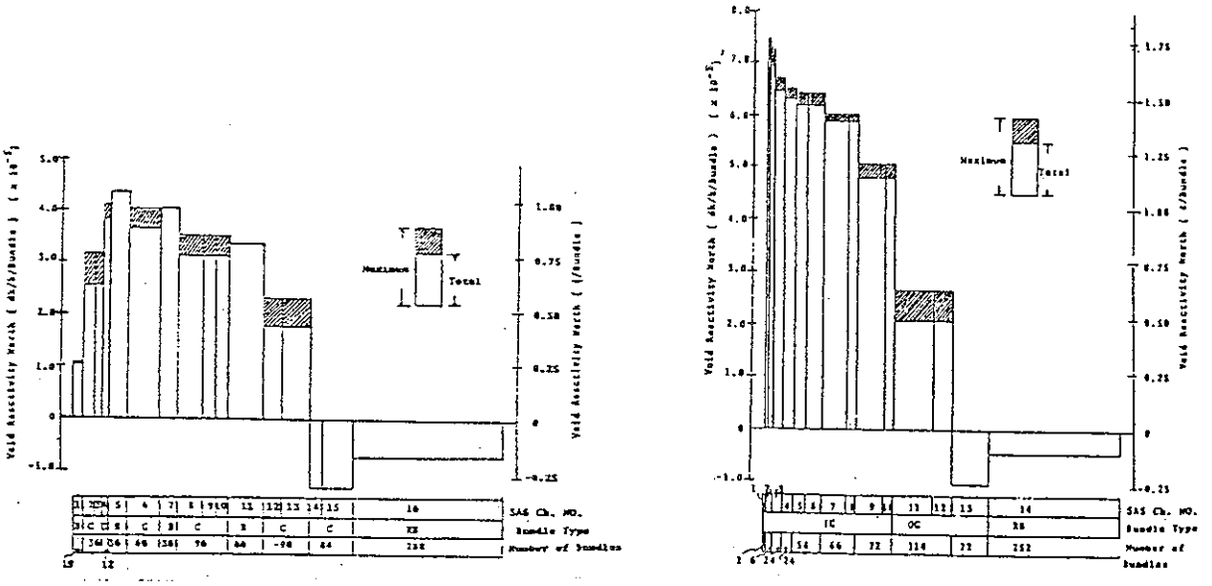

Fig. 3 Void Reactivity Worth Distribution

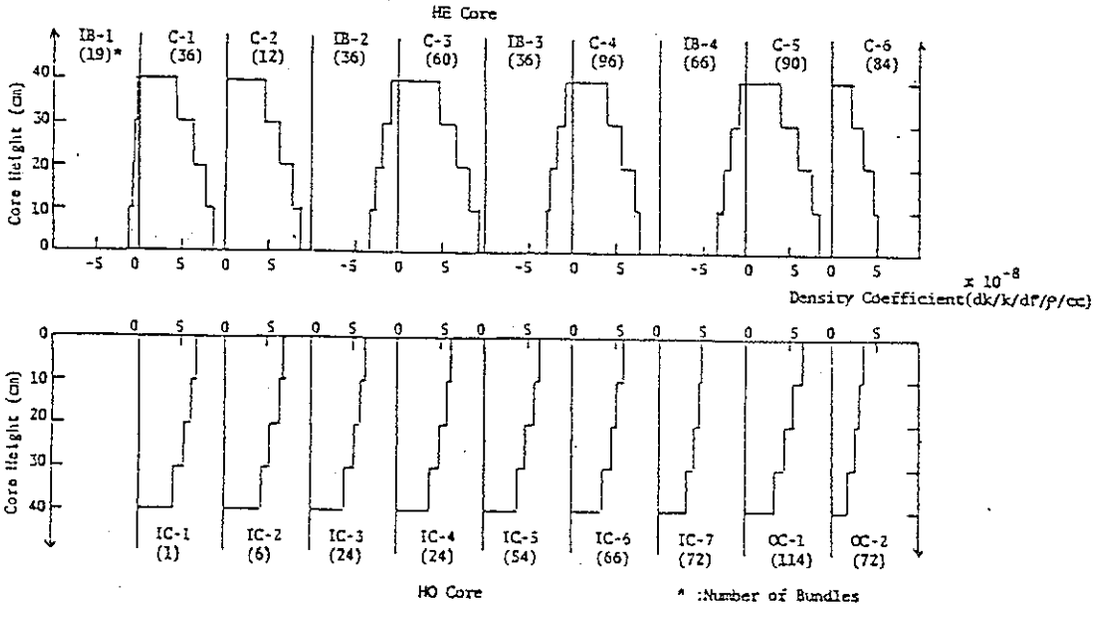

Fig. 4 Density Coefficients of Fuel in Both Cores

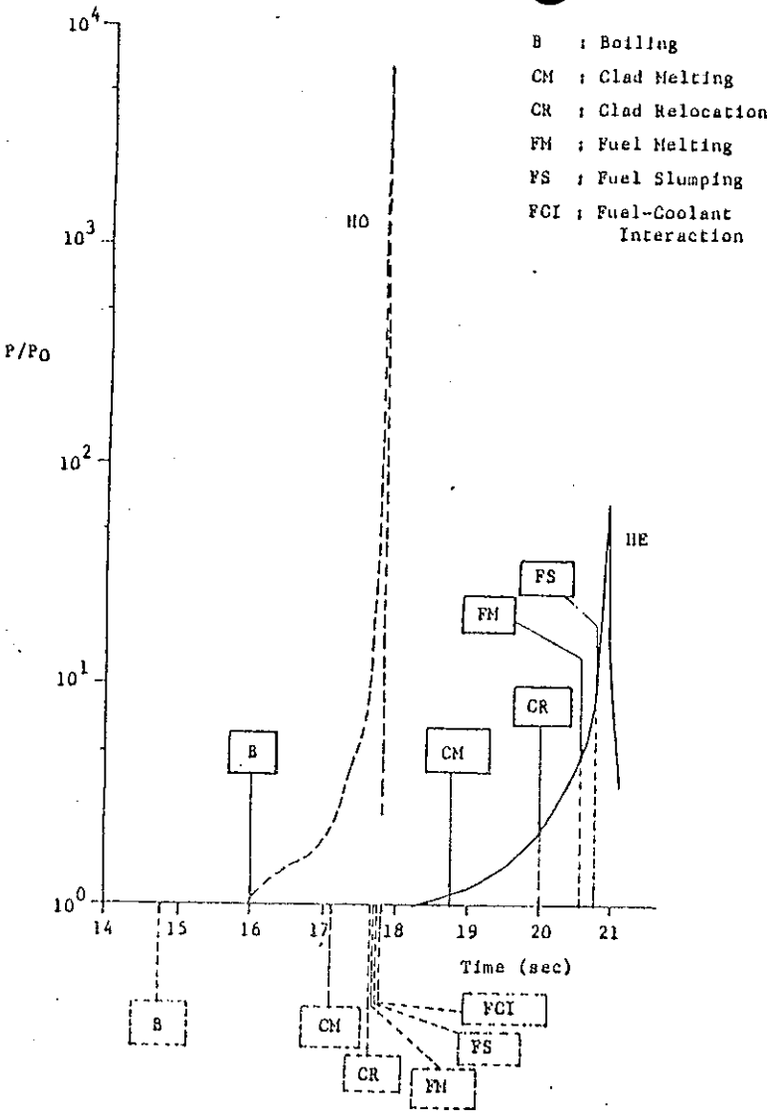

Fig. 5 Comparison of Power Traces and Accident Sequences between Heterogeneous and Homogeneous Cores in LOF Base Case

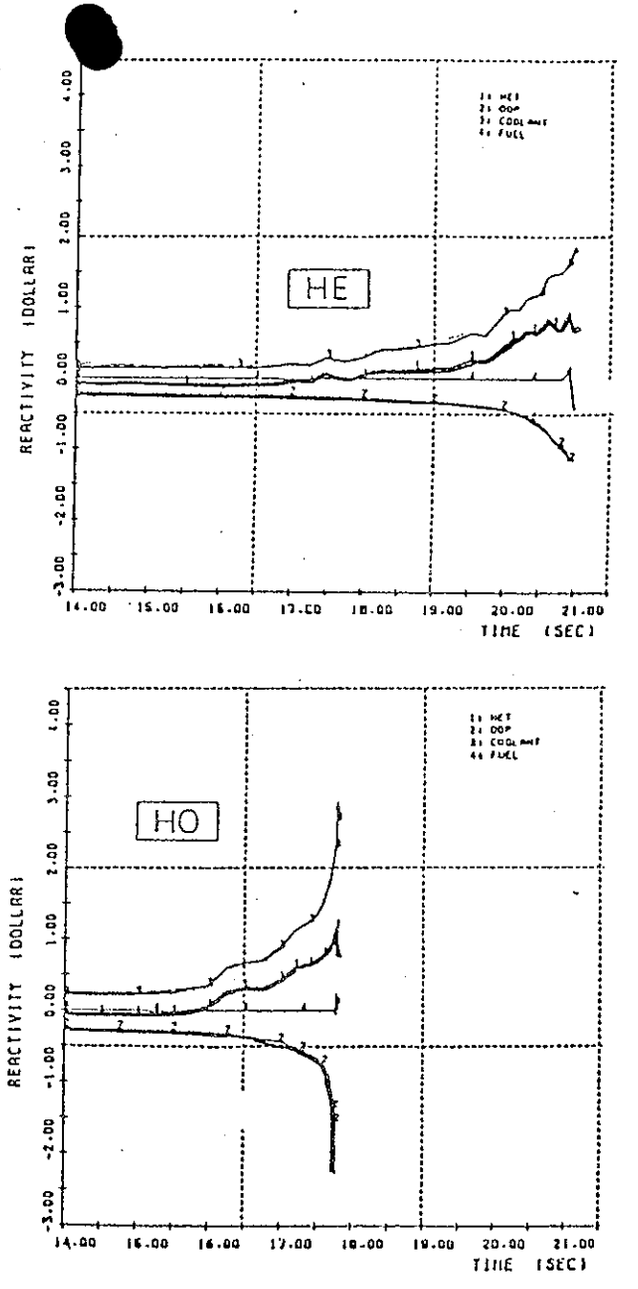

Fig. 6 Comparison of Reactivity Traces between Heterogeneous and Homogeneous Cores in LOF Base Case

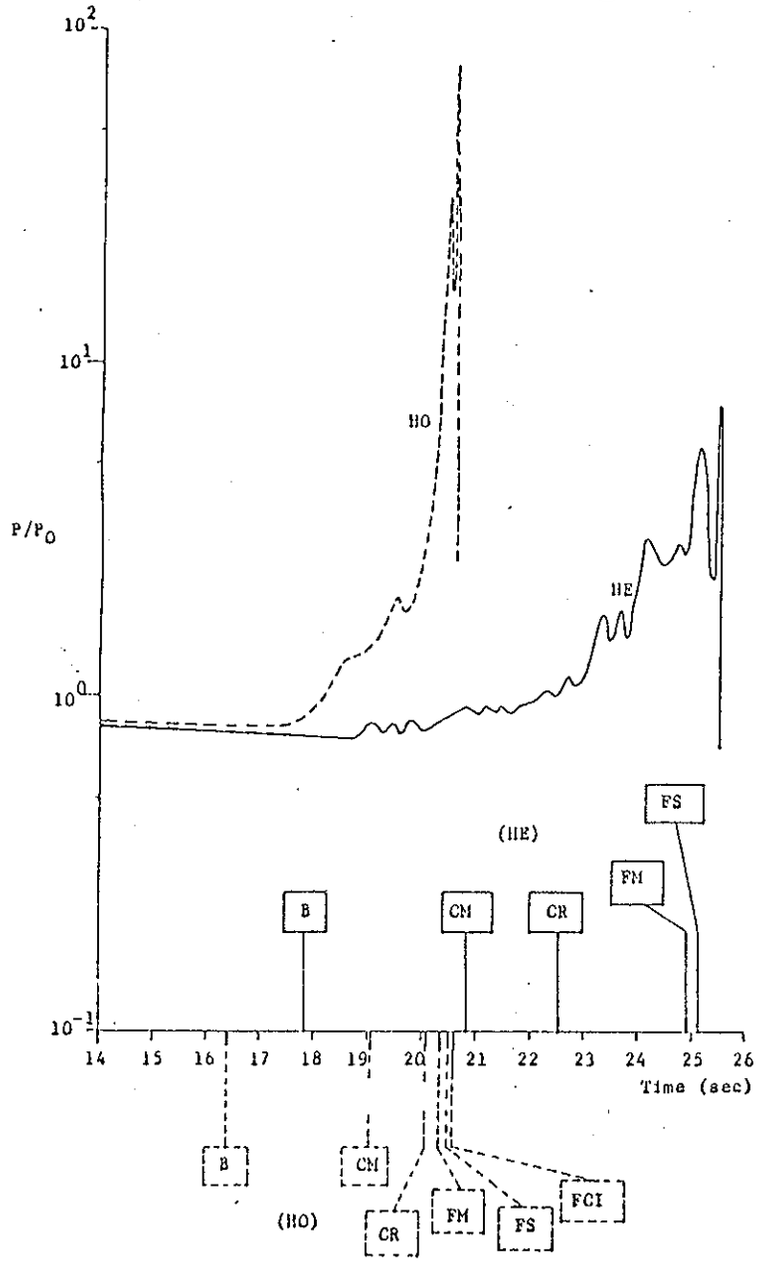

Fig. 7 Comparison of Power Traces and Accident Sequences between Heterogeneous and Homogeneous Cores in LOF Realistic Case

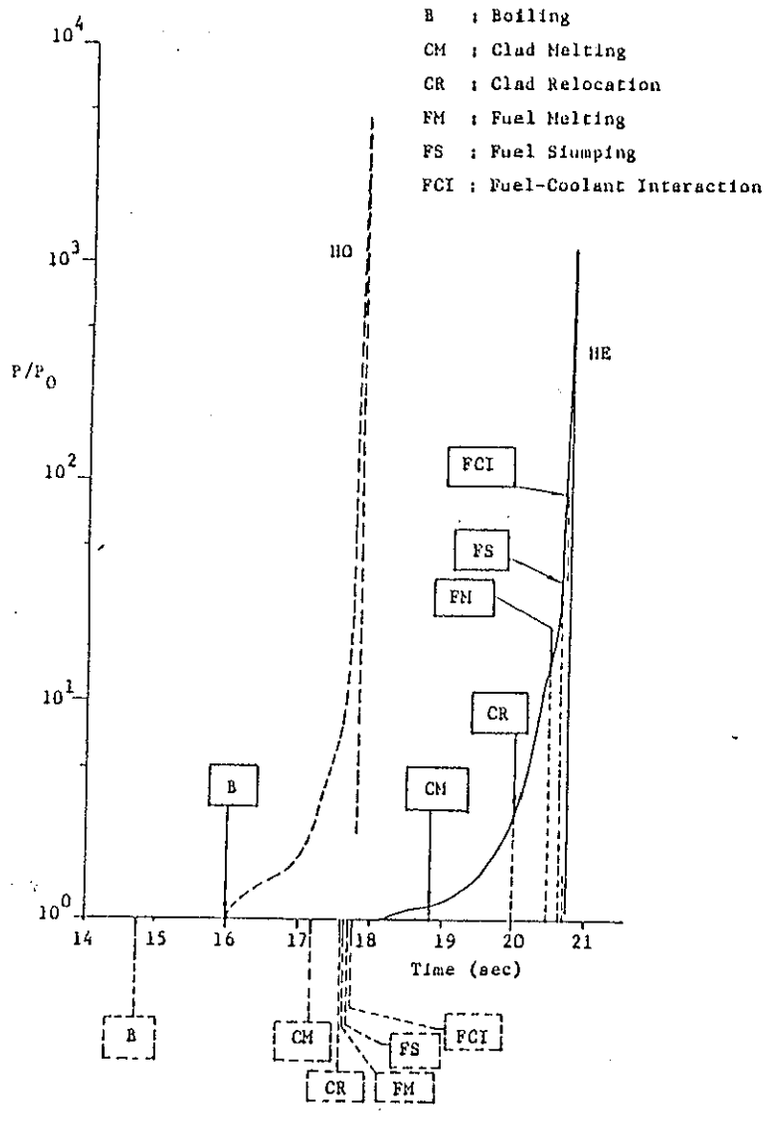

Fig. 8 Comparison of Power Traces and Accident Sequences between Heterogeneous and Homogeneous Cores in LOF Slumping Case

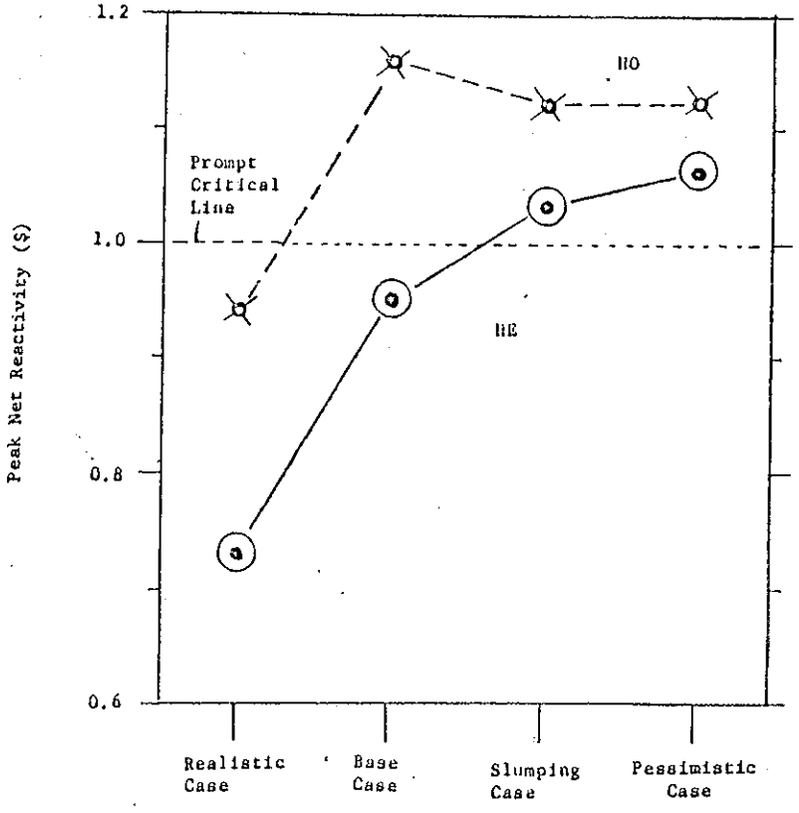

Fig. 9 Peak Net Reactivities for LOF Cases in Both Cores

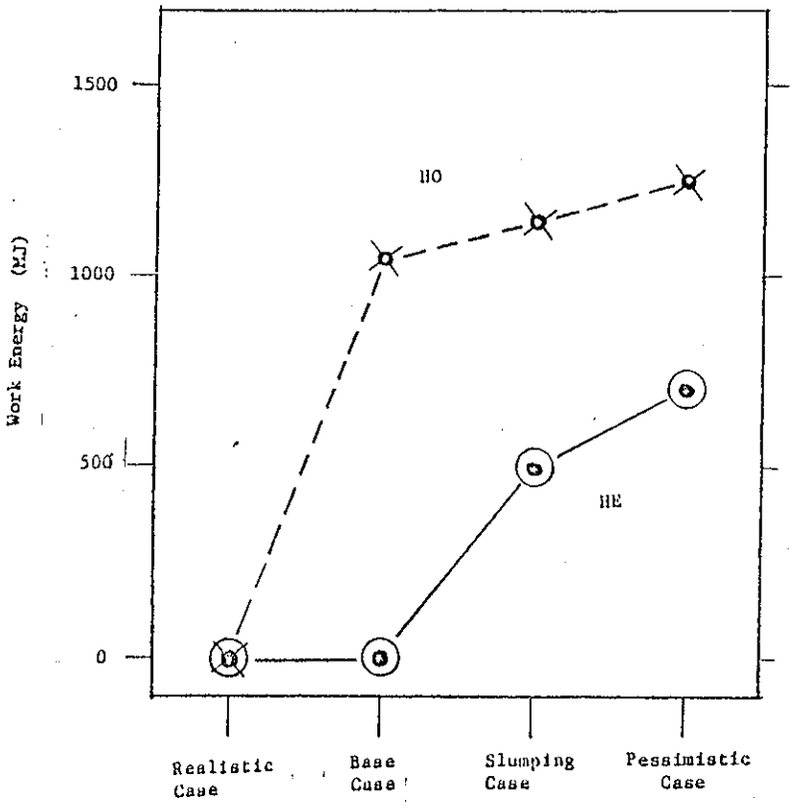

Fig. 10 Work Energies for LOF Cases in Both Cores